J-Researchers

Journal of Civil Engineering Researchers

Journal homepage: www.journals-researchers.com

3D Free Vibration Analysis of Nanocomposite Beams Carbon Nanotube Reinforced FGM Using DQ Method

Kouros Nekoufar,[a,*] Shahrzad Farrokhi [a]

[a] *Associate Professor, Department of Mechanical Engineering, Cha.c., Islamic Azad University, Chalus, Iran*

ABSTRACT

Beams are always noteworthy as an engineering structure due to their wide application in industry such as bridges, railway tracks, floors and ceilings of buildings and many other cases. Therefore, considering the wide application of these materials in industry, the analysis of this category of structures becomes important in the overall design process of these parts in a structure. With the increasing use of beams in industry and the need to increase their efficiency and ensure their proper functioning, the use of new materials such as functionally graded materials has increased. The use of composite materials, shape memory alloys, piezoelectric materials, etc. and the expansion of the scope of use of these materials has led to increased efforts by researchers to achieve the construction and design of structures and parts with better efficiency and quality. On the other hand, conducting experimental analyses on these materials is associated with problems such as size, price, complexity of the laboratory model, etc., hence the presentation of general theoretical models. In this research, the vibration analysis of a nanobeam is considered. Unidirectional FGM (functional properties along the beam thickness) with carbon nanotubes and a layer Metal and ceramic supports on various types of supports Sometimes. The solutions, including simple, complex, etc., were discussed. The solution method in question was the mixing method, and in line with the thickness of the numerical method, the differential function. It has been DQ based on this, relationships have been extracted regarding how to increase the natural frequency and the lowest natural frequency, as well as the length-to-thickness ratio, natural frequency changes, and dimensionless natural frequency changes in the beam.

ARTICLE INFO

Received: March 6, 2025
Accepted: May 22, 2025

Keywords:
Nanocomposite
Carbon Nanotube
Method GDQ
FGM
Eshelby-Mori-Tanaka method

DOI: 10.61186/JCER.7.2.21
DOR: 20.1001.1.2538516.2025.7.2.3.1

1. Introduction

Currently, the use of functionally graded nanobeams, plates, and layered structures is expanding significantly in industry. In this way, the bending stiffness and strength of functionally graded nanobeams exceed the bending stiffness of each of its components alone, which is achieved at the lowest possible weight of this type of structure ¬are usually used somewhere¬. Weight is a critical factor, meaning that the weight of the structure must be low. For example, in the aerospace, mining, and sports equipment industries. In recent years, much attention has been paid to the development of nanostructures with functionally graded properties and their applications. The general

* Corresponding author. Tel.: +98 912 525 86 98; e-mail: kouros.nekoufar@iau.ac.ir (Associate Prof. Kouros Nekoufar).

properties of these structures are high thermal resistance, high strength-to-weight ratio, good sound and energy absorption, and often low production costs. These structures have a very good light-stiffness ratio. Many applications of nanostructures with functionally graded properties require the production of complex shapes, which has made the analysis of these materials more complex. Also, to make the structure lighter and structures that require high bending stiffness, nanomaterials with functionally graded properties are used in structures. A nanocomposite is also a composite in which one or more components have dimensions less than 100 nanometers. Nanocomposite are composed of two phases. The first phase is a crystalline structure, which is actually the base or matrix of the nanocomposite and may be made of polymer, metal or ceramic. The second phase is particles on the nanometer scale. May they be Title: Filler Reinforcement for specific purposes such as strength, resistance, electrical conductivity, magnetic properties, and... are distributed within the first phase (base material).

1.1. Functionally graded materials

Functionally graded materials are composite materials that are microscopically heterogeneous and in which the properties and characteristics of the material change continuously and gradually from one level to another. In these materials, the properties change as a function of position, which may occur naturally or as a result of manufacturing processes [1]. Materials generally exhibit one property, while in functionally graded materials the properties of one side are different from the other. For example, one side may have high mechanical strength and the other side may have high thermal resistance. Figure (1-1) shows the material and its properties in different structures.

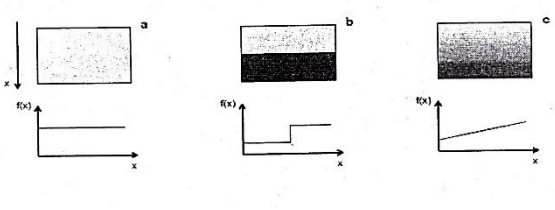

Figure 1: Types of material structures and their properties [1]

As can be seen in Figure 1, in the structure (a) the material is homogeneous and the properties are the same at all points of the material. In the structure (b) a new material is obtained by joining two materials together and the properties of the new material change in the form of bridges. Also, a boundary is created at the junction. In the structure (c) which is a functional graded structure, the properties change uniformly from one side to the other, and no boundaries can be determined between the constituent materials within the material.

So in graded materials, there is a continuous change in properties. That is, this material is formed by bonding materials to. Individually to It is not easy to obtain both comes, because in this case a boundary is created in the material. In other words, by mixing several materials with different properties, continuous and gradual changes are created in the manufactured material without creating a boundary. Due to the continuous and gradual changes that occur in the body, this manufactured material is called a functional material. The gradual change in the properties of functionally graded materials, unlike the sudden change in discrete layered materials such as fiber-matrix composites, is used to modify the fracture performance and crack growth that is clearly visible in the intermediate surface of the composite materials. These properties and characteristics are designed by manufacturers according to the needs and uses. Examples of these characteristics include crystal structures, crystal orientation, grain diameter and boundaries, particle distribution conditions, hardness and ductility values, thermal resistance, etc., which can be in any direction (horizontal or vertical). In the simplest FGMs consist of two different material components. Continuously from one to the other, as in Figure.2a it is explained that the composition of the materials can also change.

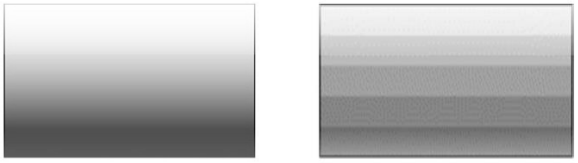

(a) (b)

Figure 2: Different designs in functionally graded structures [1]

Discontinuous face and step by step (Figure 2(b)). Both of these cases are considered structurally FGM. The basic idea of this structure was first presented in 1972 for composites and polymeric materials, and various models for the composite components in polymerization were proposed with possible applications for hierarchical structures. However, until 1980 there was no real investigation and research on how to build and evaluate hierarchical structures.

Functionally graded materials are also found in nature. It is found in the biological tissues of plants and animals and even in our own bodies, such as bones and teeth. Bamboo, oysters, and coconuts are good examples. Both bamboo and oysters are very hard on the outside and soft and durable on the inside. On the other hand, bamboo plants have other good qualities. They are lightweight, strong, and flexible. It organisms have a very suitable structure for living in the environment. All living things in

nature are best created with structures and tissues that include functional materials.

In Figure 3Cross section of a clam shell It is shown. The continuous change of material on the surface of this shell is clearly evident in its appearance. The variety of material and its relationship to appearance is noteworthy. Teeth, shells, bone Example There are studies that show how nature shapes the microscopic structure of materials by placing stronger elements where stress and strain are highest. It is, it gives order.

Figure 3: Cross section of an oyster shell [1]

The basic idea of hierarchical structures was first proposed in 1972 for composites and polymeric materials, and various models for the components of the composite in polymerization were proposed with possible applications for hierarchical structures. However, it was not until 1980 that there was any real investigation and research into how to design, fabricate, and evaluate these structures.

Functionally graded materials were developed around 1984. Two researchers, one studying aeronautics and astronautics and the other advanced materials, worked together on spacecraft. The outer shell of spacecraft is exposed to very high temperatures (about 1700 degrees), so it needs to be able to withstand the harsh conditions of the large temperature difference between the inside and outside. No single material could withstand such conditions. The researchers came up with a concept called functionally graded materials. (FGM) thought of producing a material for spacecraft bodies by gradually changing its properties, which would have both enhanced thermal resistance and good mechanical properties. They decided to use ceramics for the external surface exposed to very high temperatures and heat-conducting materials for the internal surface. This was the beginning of research activities on functionally graded materials. In 1987, their research The research project on functionally graded materials became a major project of the Ministry of Science and Research. Between 1987 and 1991, the research project It was started when many researchers from universities, laboratories and companies participated in the work. They discussed the development methods of functionally graded materials and the production steps such as material design, production and evaluation. Finally, the thermal stress-releasing material (FGM) was developed. In 1990, the first international conference on functionally graded materials was held in Sendai, Japan, and in 1992, functionally graded materials (FGM) were announced as one of the top ten technologies and attracted much attention worldwide.

1.2. Relationships governing functionally graded materials

Consider a case where the sheet is made of a material with a functional property of ceramic and metal. The material properties vary continuously along the thickness according to the following relationships:

$$E(z) = E_m + E_{cm}V_f(z) \quad (1)$$
$$\nu(z) = \nu_m + \nu_{cm}V_f(z)$$
$$\rho(z) = \rho_m + \rho_{cm}V_f(z)$$
$$\mathrm{E_{cm}} = \mathrm{E_c} - \mathrm{E_m}$$
$$\nu_{\mathrm{cm}} = \nu_{\mathrm{c}} - \nu_{\mathrm{m}} \quad (2)$$
$$\rho_{\mathrm{cm}} = \rho_{\mathrm{c}} - \rho_{\mathrm{m}}$$

Which refers to materials with the properties of metals and ceramics and $V_f(z)$is the volume fraction of structural materials is most often expressed by power law or sigmoid functions. For power-functionally graded materials, the volume fraction is expressed as:

$$\mathrm{V_f}(z) = \left(\frac{z}{h} + \frac{1}{2}\right)^N \quad (3)$$

Where *N* represents the power law, the material index, which shows the index of change of the material in its thickness.

For sigmoid functionally graded materials, the volume fraction function is expressed as follows:

$$\mathrm{V_f}(z) = \begin{cases} 1 - \frac{1}{2}\left(1 - \frac{2z}{h}\right)^N & 0 \le z \le \frac{h}{2} \\ \frac{1}{2}\left(1 + \frac{2z}{h}\right)^N & -\frac{h}{2} \le z \le 0 \end{cases} \quad (4)$$

Similarly, *N* represents the thickness change profile of the material, which controls the change in Young's modulus.

For two-layer functionally graded materials:

$$\mathrm{V_f}(z) = \begin{cases} \left(1 - \frac{2z}{h}\right)^N & 0 \le z \le \frac{h}{2} \\ \left(1 + \frac{2z}{h}\right)^N & -\frac{h}{2} \le z \le 0 \end{cases} \quad (5)$$

There is another type of functionally graded material in which the material properties follow an exponential distribution and are expressed as follows:

$$E(z) = E_m e^{\frac{1}{h}\ln\frac{E_c}{E_m}(z+\frac{h}{2})} \quad (6)$$
$$\nu(z) = \nu_m e^{\frac{1}{h}\ln\frac{\nu_c}{\nu_m}(z+\frac{h}{2})}$$
$$\rho(z) = \rho_m e^{\frac{1}{h}\ln\frac{\rho_c}{\rho_m}(z+\frac{h}{2})}$$

The exponential change model of properties in functionally graded materials is a suitable model for obtaining an accurate solution of elasticity.

1.3. History of studies

In 2001, Sankar, a bullet from the barrel–Bernoulli made of materials FGM with simple supports has been statically investigated. An orthotropic beam is under normal stress only and all desired elastic parameters are proportional to which is constant and z is the coordinate component in the thickness direction which has obtained the exact solution. (The beam is only mechanically loaded in a sinusoidal form and Poisson's ratio is assumed to be constant). [3]

In 2002, Chakraborty and his colleagues used the finite element method based on the first-order shear deformation theory to calculate the change in elastic and thermal properties through the thickness. Both exponential and power-law deformations of the material properties were used to represent the changes in different stresses. (The beam was considered under both thermal and mechanical forces.)). [4]

In 2003, Chakraborty and his colleagues used a finite element method based on the first-order shear deformation theory to study the effects of geometric nonlinearity on the dynamic and static response of isotropic, composite, and material beams. FGM has been used. The general Lagrange equation of the linear beam element for the displacement analysis and rotation Big ones to the work has been done. Both frequencies High and low pulse Loading curves are used to show the nonlinear effect on the transient response. (Power distribution is considered for material properties.) [5]

In 2004, Shi and colleagues, Analytical solution of a single-ended piezoelectric beam made of materials FGM has been studied under different loads. A piezoelectric beam with a continuously varying elastic parameter and material density is considered. A pair of stress and induction functions are assumed and determined as polynomials. Based on these functions, a set of solutions of this paper is obtained. Such as problems such as a piezoelectrically engaged one-ended beam with a constant body force or without body force, etc. In this research, the direct and inverse behavior of a piezoelectrically restrained one-ended beam is investigated. The Airy stress function method is used to find the solution. The result is that the stress function used to analyze a one-ended beam made of FGM materials and piezoelectric layers is similar to the function used for a similar beam made of homogeneous elastic materials. Also, if the body forces are ignored, some effects such as the effect of the FGM material parameter and layers are eliminated in the analytical solution. [6]

In 2006, Ding and his colleagues have investigated the plane stress problem of non-isotropic beams, assuming that the desired elastic parameters are arbitrary functions of the thickness coordinate direction. Partial differential equations, which are expressed by the Airy stress function for the plane problem of materials the non-isotropic FGM is satisfied and includes body forces. The solutions performed are: solution for beam under pure tension and bending, solution for single-ended fixed beams with free ends under shear force, solution for single-ended fixed beams or beams with simple supports under uniform force, solution for double-ended fixed beams under uniform force and solution for beam under body force and can be easily solved. The elasticity values for homogeneous beams decrease. In this case Research the Silverman 1964 method has been generalized to provide a general way of obtaining the stress function for beams made of materials with non-isotropic functional properties. No assumptions are made for the variation of the desired elastic quantities through the thickness. In addition, the change in physical force with coordinates has been taken into account.[7]

In 2007, Kapoor and his colleagues third-order zigzag theory based on a model for beams made of materials layered FGM in combination with the modified law of mixtures for effective elastic modulus have been validated with tests for free and static vibration response.

Two sets, using powder metallurgy and technique respectivelyAl/sicNi/〖AL〗_2 O_3Heat dissipation generated are being considered for validation effect of number of layers the accuracy of the theoretical model is discussed. A finite element model for dynamic analysis of material beams with layered functional properties, efficient zigzag theory for layer mechanics, modified mixed method the elastic modulus effect has been estimated and validated in laboratory experiments. Two models of three-layer and five-layer materials have been used FGM has been used for calculations. The volume fraction of the material is assumed to be it varies exponentially along the thickness slow.[8]

In 2007, Kaduli and his colleagues developed a displacement field based on higher-order shear deformation theory to study the static behavior of beams made of materials. Metal-ceramic FGMs are used under ambient temperature. Beams made of materials FGM with varying metal and ceramic volume fractions are considered based on the power law. Using the static potential energy law, the finite element form of the static equilibrium equation for a beam made of FGM materials is shown. Numerical results of vertical deflection and axial and shear stresses in a thick FGM beam in equilibrium under uniform load distribution for clamped boundary conditions–The effect of power distribution for different metal compositions is discussed. – Ceramic beam made of materials with FGM on deflection and stresses has been

explained. The study reveals that the static deflection and static stresses will not be the same depending on whether the load is applied to a pure metal or pure ceramic surface. [9]

In 2007, Lee, an integrated method (analytical solution) for static and dynamic analysis of beams made of materials FGM, considering rotational inertia and shear deformation. All material properties are optionally considered as a function of the beam thickness. The results obtained cover the homogeneous Timoshenko beam with fixed elements without material properties. The proposed method for laminated Timoshenko beams is applicable to they are used the equations are obtained assuming the Timoshenko theory. It is assumed that the shear deformation and deflection in the direction Z depend only on X and temperature and are constant at any cross section. Numerical results for a beam that obeys a power law Multilayer Euler-Bernoulli and Timoshenko beams and beams obtained w When shear deformation and rotational inertia are Simultaneously disregarded, Euler's results–Bernoulli gets Come.[10]

In 2007, Tao and his colleagues used the Airy stress function method for a piezoelectric single-ended beam made of materials with functional properties. It is assumed that the feature t the mechanical and electrical properties of the material have similar variations along the thickness. and, a two-dimensional plane elasticity solution for coupling of electric fields–The elasticity of the beam under different loads has been obtained. This solution is for analyzing a beam made of functional materials with a layer Piezoelectric material with optional changes in properties. The properties of the materials will also be affected. Material properties with functional properties on the structural response of the beam under various loads have been studied in numerical examples. (A single-ended beam with a free end under a uniform load on the upper edge is assumed).[11]

In 2007, Chen His colleagues have investigated the bending problem of a non-isotropic single-ended beam made of a material with linearly distributed functional properties under load. Analysis based on exact elasticity equations for plane stress problems. The stress function is given by the form of a polynomial function of the longitudinal component is introduced.[12]

The analytical solution shows a good agreement compared to the finite element calculations. The desired elastic parameters are functions of the beam thickness only. The analytical solution can be easily reduced to the solution for a homogeneous beam.

In 2007, Chen and colleagues investigated the bending problem of a non-isotropic single-ended beam made of functionally-proper materials under thermal and uniform spread loads. are, where the material parameters are functions of the thickness coordinates. The thermal conductivity problem behaves like a one-dimensional problem along the thickness. Based on the initial equations for the plane stress problem, The stress function is the form of a polynomial function of the longitudinal coordinates in such a way that the stress it is assumed that they are obtainable.[13]

In 2007, Chen and his colleagues presented an exact solution for the bending and free vibration of a beam made of functional material on an elastic base based on the two-dimensional elasticity theory. The beam is assumed to be orthotropic at all points, while the material properties vary exponentially throughout the thickness. The system of governing partial differential equations is reduced to a normal state in the thickness limit by expanding the state variables into a series. Infinite sinusoidal waves decrease. The problem is finally solved using the state space method.[14]

In 2007, Zhong His colleagues, an elasticity solution for beam bending FGM using inverse methods in Airy stress function sentences was reported. [15]

In 2007, Ding and his colleagues, a series of analytical solutions for beams anisotropic FGM with various support conditions were extracted using an Airy stress function in general polynomial form. [16]

In 2009, Farhatnia and his colleagues developed analytical and numerical solutions for beams FGM under stress. They presented thermomechanical equations; they used the Euler-Bernoulli beam theory for analytical solution and the finite element method for numerical solution.[17]

In 2010, Ali Bigelow Thermoelasticity analysis for the beam FGM with integrated piezoelectric surfaces is presented, the properties in the thickness direction are assumed to be exponential and the Poisson's ratio is assumed to be constant. Beam in the support condition. Sometimes simple, with a limited length, and subjected to uniform pressure and thermal force, and in a state of plate tension. It is and at its lower level the temperature is considered to be zero.[18]

In 2010, Shimshak Beam base frequency analysis FGM with theory examined various higher-order [19]

In 2012, Tai and colleagues, beam bending and vibration FGM with theory various higher-order shear deformation models were investigated.[20]

In 2013, the Pardahan and his colleagues, free vibration of the beam Eulerian and Timoshenko investigated the FGM using the Rayleigh-Ritz method. [21]

In 2013, Thomas and his colleagues, a nanocomposite beam FGM with nanotubes. They modeled randomly placed beams using finite elements and investigated their free vibrations. For this analysis, Timoshenko beam theory was used. Also, Mori Tanaka approach was used to analyze the beam properties and the equations of motion were extracted using Hamilton's laws. The obtained results

provide the most accurate representation of the nanotube placement. [22]

In 2013, Mohammadi Mehr and his colleagues analyzed the bending and vibration of a nanocomposite beam with functional properties based on the Timoshenko beam model based on coupled stress theory. The equations of motion were obtained using Hamilton's theory and Navier equations, and the functional properties FGM is considered as exponential functions.[23]

In 2013, Heshmati and his colleagues performed the free vibration analysis of a nanocomposite beam with carbon nanotube fibers with functionally graded properties using the Ashleby, Mori, Tanaka approach. In this project, the governing equations were derived based on the virtual work rules and assuming the Euler-Bernoulli beam theory. The finite element method was also used for better approximation. [24]

In 2015, Moradi Dastjerdi and colleagues performed vibration analysis for a composite beam. FGM reinforced with carbon nanotube fibers and placed on an elastic substrate. For the analysis of free vibrations, shear deformation theory was used and the equations of motion were obtained using Hamilton's energy laws and Navier's method. The substrate considered in this project is the classical Winkler-Pasternak substrate and the functional properties of the materials are in the thickness direction and the placement of the nanotubes carbon nanotubes were prepared according to Mori Tanaka principles. [25]

Zarehparvar-Shoja et al. [26], utilizes carbon nanotubes, to improve the mechanical characteristics of concrete as a building material.

2. Method of square differences

Numerical method of square differences It is a numerical method for solving differential equations. It was first introduced by Bellman and his colleagues before 1970. It approximates the derivatives of a function at each location by a linear series of all the values of the function at the sample points. The key to the method is the use of the method of square differences in determining the weighting coefficients. Bellman initially proposed two methods for calculating the weighting coefficients for first-order weighted derivatives. The first method is based on a system of algebraic equations of anomalous conditions. and the second method uses a simple algebraic formulation, but the coordinates of the points are determined by the roots of the Legendre polynomial. The method of square differences has been used as a powerful numerical discretization tool. Compared to the finite difference method Low order and finite element methods The square difference method produces much more accurate results with fewer node points, resulting in fewer calculations.

2.1. Introduction to the method of square differences and its governing equations

Many engineering problems or sets of partial differential equations It is accompanied by appropriate boundary conditions. For example, Newton's laws in fluids are modeled by the Navier-Stokes equations, the vibration of thin shells is modeled by fourth-order differential equations, and also waves acoustics and micro can be solved by the Helmholtz equation Model. In the usual case, solving such differential equations directly is a very difficult task. The method of square differences for similar the modeling of incompressible viscous flow, free vibration of beams, plates, and shells, and wave analysis in one and multidimensional domains, in Cartesian and curved coordinates, have been applied by Xu Cheng and his colleagues.

In most cases, approximate solutions are computed using function values at a series of sample points. At this point, the question may arise as to what is the relationship between partial differential equations and function values at sample points. In fact, it seems that there should be a bridge between them. The numerical gridding technique is in fact the bridge between the two.

Currently, there are many numerical techniques available. Among them, we can mention methods such as finite difference, finite element, and finite volume. The finite difference method is based on the use of Taylor expansion or polynomial approximation, while the finite element method uses the calculus of variations. and weighted residuals are used. In the finite volume method, the direct application of the stability principle to the cells is used. To achieve an acceptable accurate answer, in many of the numerical solutions mentioned, the number of sample points can be increased. Vibration analysis can be used as an example for this. Of course, it should be noted that in many problems, applying a larger number of sample points is necessary to achieve an accurate answer with high accuracy, which is one of the disadvantages of these methods. To solve many problems, a series of differential equations must be solved, the analytical solution of which is difficult and complex. Therefore, approximate methods must be used. In most cases, the approximate solution is expressed by a series of function values at certain points (node points or grid points).

The method of square differences is a numerical method with high accuracy while the number of nodes points it considers is less than other numerical methods. In this method, the partial derivative of a function with respect to a coordinate direction is expressed as an algebraic sum of all the values of the function at all grid points along the

desired direction. Instead of the methods proposed by Bellman, other researchers have used Lagrange's interpolated polynomials.

2.2. Approximating derivatives by the method of square differences

The method of square differences is a numerical method that approximates the derivatives of a function by a linear series. This numerical method is based on the idea of squaring the integral. It is derived from. In this section, a brief explanation of the integral squaring method is first given, and then the method of square differences is examined. One of the problems that usually arises in engineering problems is the measurement and calculation of $\int_a^b f(x)dx$ In the distance*[a,b]*. If there is a function *F* such that it is, then the value of this integral will be equal to *F(b)-F(a)*. Unfortunately, in many engineering problems it is very difficult or impossible to find the function *F*. Instead, in many problems only the values of f are known in the interval, in which case a numerical method is necessary $df/\mathrm{dx} = F$.

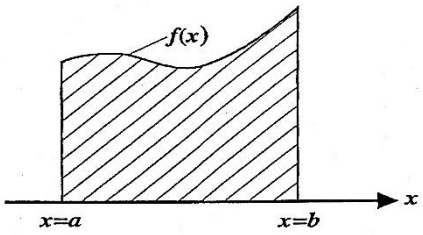

Figure 4: Calculating the integral of a function f(x)In the interval[a,b]

On the other hand, the integral of the function f(x)In the interval [a,b] represents the area under the curve of the function f(x). Therefore, calculating this integral is equivalent to approximating the area under the curve. Using this simple principle, various numerical methods have been introduced. In general, the approximation of this integral is represented in the following form:

$$\int_a^b f(x)dx = g_1 f_1 + g_2 f_2 + \cdots + g_N f_N = \sum_{k=1}^{N} g_k f_k \quad (7)$$

in which g_k the weighting coefficient functions and the f_k are the values of the function f at the points X_k. The equation mentioned is called the integral square, which is used to calculate the integral of the function. Now we will examine the differential squaring method.

Consider a one-dimensional problem, as shown in Figure (4). It is assumed that the function *f(x)*It has good uniformity at all points of the range.

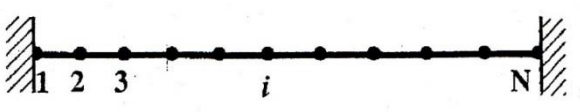

Figure 5: A one-dimensional problem

Using the idea of integral squaring, Bellman proposed in 1972 that the first-order derivatives of the function f(x)At the nodes Xi, can be approximated by a sum of function values over the entire domain as follows.

$$f_x(x_i) = \left(\frac{df}{dx}\right)_{x=x_i} = \sum_{j=1}^{N} g_{ij} \cdot f(x_i) \quad , \text{ for } i = 1,2,\dots,N \quad (8)$$

in which g_{ij} weighting coefficients and Nis the number of sample points in the entire domain. The above equation is a differential quadrature equation or it is called DQ. It should be noted that the weight coefficients are different at different positions of Xi. Therefore, the key to solving the differential quadrature approximation is to determine the weight coefficients. So, in the method of square differences, to find the unknown of the differential equation, the derivatives of the function are considered to be equivalent to the sum of a series of products of the weight coefficients at certain points of the function and then the unknown is obtained from solving the system.

The main relationship of the method of square differences is generally defined as follows:

$$\left(\frac{\partial^n f(x)}{\partial x^n}\right)_{x=x_i} = \sum_{r=1}^{N} g_{ir}^{(n)} \cdot f(x_r) \quad (9)$$
$$n = 1,2,\dots,N \quad , \quad i = 1,2,\dots,N$$

in which f is the desired function, N is the number of sample points, Xi is the i-th sample point of the function interval, and g_{ij} is the weighting coefficients for the derivative. Therefore, it can be seen that two very important and determining factors in the accuracy of the square difference method are the weighting coefficients and the selection of sample points, which will be mentioned below.

2.2.1. Selecting sample points

The method of selecting sample points is one of the most important parameters affecting the accuracy of the answers. There are several methods for selecting sample points, three of which will be mentioned here.

a) Sample points with equal distances

The first and simplest method for selecting sample points is to define the scope of the problem as N the point should be divided by equal distances. That is:

$$\Delta x = x_2 - x_1 = x_i - x_{i-1} = x_N - x_{N-1} \quad (10)$$

The division is done using the following relationship:

$$x_i = a + \left[\frac{i-1}{N-1}\right](b-a) \quad (11)$$
$$i = 1,2,\dots,N \quad , \quad a \le x_i \le b$$

3. Roots of Chebyshev polynomials

Usually, choosing points with equal distances does not yield accurate results. Experience has shown that choosing sample points with unequal distances gives accurate answers. The use of orthogonal polynomial roots is one of the common methods for selecting sample points with unequal distances. For example, Chebyshev polynomial roots are widely used in solving lubrication problems and orthotropic plates. In the field of using orthogonal polynomial roots, extensive studies were conducted by Kwan and Chang in 1989, during which it was shown that in the field of solving chemical engineering problems and applying the method of square differences, using Chebyshev polynomial roots as sample points leads to better results. On the other hand, Malik, in 1993, showed that using Legendre orthogonal polynomial roots is more useful than Chebyshev polynomials in solving elasticity and plate problems. In any case, depending on the type of problem, one of the mentioned methods can be used to select sample points.

The division using Chebyshev polynomials is as follows:

$$x_{\mathrm{i}} = \left[\mathrm{a}, \mathrm{a} + \frac{1}{2}(1 - \cos\left[\frac{2\mathrm{i} - 1}{2\mathrm{N}}\right])(\mathrm{b} - \mathrm{a}), \mathrm{b}\right] \quad (12)$$

$i = 2,3, \dots, N-1 \;\; , \;\; a \le x_i \le b \;\; , \;\; x_l = a \& x_N = b$

Roots of Legendre polynomials:

In order to divide the interval using the roots of the Legendre polynomial, first the polynomial of degree. We define n of the Legendre function:

$$\mathrm{p_n(x)} = \frac{1}{2^{\mathrm{n}}\,\mathrm{n!}}\left[\frac{\mathrm{d^n}}{\mathrm{dx^n}}(\mathrm{x}^2 - 1)^{\mathrm{n}}\right] \quad (13)$$

And the division of points with this method will be using the following relations:

$$x_{\mathrm{i}} = \left[\mathrm{a}, \mathrm{a} + \frac{1}{2}(1 - \cos\left[\frac{(2\mathrm{i} - 1)\pi}{2\mathrm{N} - 4}\right])(\mathrm{b} - \mathrm{a}), \mathrm{b}\right] \quad (14)$$

$i = 2,3, \dots, N-1 \;\; , \;\; a \le x_i \le b \;\; , \;\; x_l = a \& x_N = b$

What is observed in these relations is that the density of the number of nodes at the two ends of the interval is more than in the middle, which leads to better results. Of course, one of the shortcomings of the mentioned polynomials is that they do not include the beginning and end points of the interval, while in many engineering problems there is a need to apply boundary conditions at the beginning or end points of the interval.

In 1992, in two papers examining fluid mechanics problems and solving Navier-Stokes equations, Shaw and Richards proposed a formula that, in addition to selecting sample points with unequal distances, also includes the beginning and end points of the interval:

$$x_i = \left[\frac{1}{2}\left(1 - cos\left[\frac{(i-1)\pi}{N-1}\right]\right)\right] \quad (15)$$

$i = 1,2, \dots, N \;\; , \;\; a \le x_i \le b \;\; , \;\; x_i = a \, , x_N = b$

Of course, it should be noted that in problems whose derivatives the higher the order, the more sample points are needed.

4. Selecting the weighting coefficient function

When the weight coefficients were first determined, a bridge was established to connect the derivatives in the governing differential equations and the function values at the sample points. In other words, with the weight coefficients, the function values can easily be used to calculate its derivatives. To apply the differential squaring method to solve a differential equation, we must write the derivatives as the matrix product of the weight coefficients in the vector of unknowns, as mentioned above. Therefore, we must look for a solution to obtain the matrix of weight coefficients. Various methods have been proposed to calculate the matrix of weight coefficients. In these methods, first the function f_A known function is assumed. By taking the derivative of this function and satisfying the equality of the right and left sides of the above equation, the weight coefficients are obtained. This function, which is used to obtain the weight coefficient function, is called the test function or experimental function. After inventing the method in 1971, Bellman introduced two ways to obtain the weight coefficient matrix. The first method was the Gauss method, which obtains the weight coefficients by solving the Vandermonde apparatus. Unfortunately, in this method, when the number of the number of sample points increases, the Vandermonde matrix conditions will become abnormal and the solution of the device will be difficult. Bellman presented his second method to solve this problem. In this method, Legendre's transferred polynomials are used. In this method, the sample points are the roots of Legendre's polynomials, which is of course a big problem in using this method because in many engineering problems, it is necessary to choose the sample points arbitrarily and freely. Considering the many problems that existed in both methods presented by Bellman, many scholars tried to solve this problem with various test functions. In the following, we will examine and define several different methods.

4.1. Bellman's first method

In the first Bellman method, the function introduced as the test function is of the following form:

$$h(x) = x^k \quad and \quad k = 1,2, \dots, (N-1) \quad (16)$$

It is clear that the above relationship N test functions are given. To find these weighting coefficients, N test

functions must be obtained at N sample points, namely $X_1,\ldots,X_N$.

By substituting this function into the original relation of square differences, we will have:

$$\sum_{j=1}^{N} g_{ij} x_j^k = k x_i^{(k-1)} \qquad (17)$$

$$k = 0,1,\ldots,(N-1) \ , \ i = 1,2,\ldots,N$$

So the number of weight coefficients per i,j=1,...,N is equal to N×N So we have a matrix N×N We have (i.e. N Equation and N unknown) which is calculated by solving a system, the vector of the weight coefficient matrix. The system of equations above has a unique solution, because its matrix is in the form of the Vandermonde matrix. Unfortunately, when N increases, the matrix is placed in an abnormal condition and it becomes difficult to find its inverse. To obtain results using this method, it is usually N it must be less than 13.

4.1.1. Bellman's second method

This method is similar to Bellman's first method, but it uses other test functions. Bellman defined another test function using Legendre's transformed orthogonal polynomials according to the following relation:

$$h_j(x) = \frac{L_N(x)}{(x - x_j) L_N^{(1)}(x_j)} \ , \ j = 1,2,\ldots,N \qquad (18)$$

So that in it N Number of sample points, $L_N(x)$ Legendre polynomial of order N and $L^{(1)}{}_N(x)$ is the first derivative of $L_N(x)$. By choosing the roots of the Legendre polynomial and using the above relation for N points, Bellman and his colleagues obtained a simple relation for calculating the weighting coefficients, which is as follows:

$$g_{ij} = \frac{L_N^{(1)}(x_i)}{(x_i - x_j) L_N^{(1)}(x_j)} \ , \ j \neq i \qquad (19)$$

$$g_{ij} = \frac{1 - 2x_i}{2x_i(x_i - 1)} \qquad (20)$$

Therefore, with the help of the above relations, calculating weight coefficients is an easy task.

As you can see in this method, unlike the first Bellman method, the selection of sample points is not free. This means that in this method, the selection of sample points is exactly based on the roots of the Legendre polynomials and is not free, whereas in many engineering problems, the selection of sample points should be completely arbitrary.

4.2. The Kwan Chang Method

To improve Bellman's methods in finding weight coefficients, many efforts have been made by researchers. One of the most important methods was introduced by Kwan and Chang. Kwan and Chang from the Lagrange median polynomial Below to they used it as a test function.

$$h_j(x) = \frac{M(x)}{(x - x_j).M^{(1)}(x_j)} \ , \ j = 1,2,\ldots,N$$
$$M(x) = (x - x_1)(x - x_2)\ldots(x - x_N) \qquad (21)$$
$$M^{(1)}(x_i) = \prod_{j=1, r\neq i}^{N} (x_i - x_j)$$

Therefore, the weighting factor in the N sample points are obtained as follows:

$$g_{ij} = \frac{1}{x_j - x_i} \prod_{j=1, r\neq i}^{N} \frac{x_i - x_r}{x_j - x_r} \ , \ j \neq i$$
$$g_{ij} = \sum_{r=1, r\neq i}^{N} \frac{1}{x_i - x_r} \qquad (22)$$

The advantage of this method over Bellman's second method was that there was no longer any restriction on the selection of sample points.

4.3. Method GDQ or Generalized Show Method

The general method of Shaw is inspired by Bellman methods. This method includes all other methods. Choosing a suitable test function that does not have two defects of Bellman functions is a very important task. One of the important parameters involved in this choice is a correct understanding of the logic governing the method of square differences and the role of the test function on these equations, because Shaw and Richards were able to achieve better results by choosing different test functions. The reason for this is that the test function is a function with the help of which we obtain the weight coefficients. By placing this function in the main formula of the method of square differences, the weight coefficients are obtained. After obtaining the weight coefficients, we use them in solving various differential equations, while the weight coefficients are extracted only for the derivative of the test function and only calculate the derivatives of the test function accurately. In fact, by using the weight coefficients obtained from the test function, we approximate the function governing the differential equation with the test function. Therefore, any test function that can better approximate other functions will result in more accurate answers. Four examples of basic polynomials are given below:

$$h_j(x) = x^{j-1} \ , \ j = 1,2,\ldots,N$$
$$h_j(x) = \frac{L_N(x)}{(x - x_j) L_N^{(1)}(x_j)} \ , \ j = 1,2,\ldots,N$$
$$h_j(x) = \frac{M(x)}{(x - x_j).M^{(1)}(x_j)} \ , \ j = 1,2,\ldots,N \qquad (23)$$
$$h_1(x) = 1 \ , \quad h_j(x) = (x - x_{j-1}).h_{j-1}(x) \ , \ j = 2,3,\ldots,N$$

in which $L_N(x)$ is a Legendre polynomial of degree N. It is also assumed that the degree of the approximation

polynomial in relation (a) is *N-1*. Among these four original polynomials, equations (b) and (c) are Newton's median polynomials. The difference between equations (b) and (c) is in the distribution of sample points. If equation (c) is defined at the sample points of the Legendre polynomial. Equation (c) becomes (b). So, in fact, equation (b) is a special case of equation (c). As a result, the weighting coefficients for the first-order derivative are obtained from the following relationship:

$$g_{ir}^{(1)} = \frac{\prod_{j=1,j\neq i}^{N}(x_i - x_j)}{(x_i - x_r)\prod_{j=1,j\neq r}^{N}(x_r - x_j)} \quad (24)$$
$$i,j,r = 1,2,\dots,N$$

Using the existing relationships, the weight coefficients for the remaining derivative orders can be obtained, which are:

$$\mathrm{g}_{\mathrm{ir}}^{(\mathrm{n})} = n\left[\mathrm{g}_{ii}^{(n-1)}\mathrm{g}_{ir}^{(1)} - \frac{\mathrm{g}_{ir}^{(n-1)}}{x_i - x_r}\right] \quad (25)$$
$$i,r = 1,2,\dots,N \quad and\ n = 2,3,\dots,N-1$$

$$\mathrm{g}_{ii}^{(n)} = -\sum_{r=1,r\neq i}^{N}\mathrm{g}_{ir}^{(n)} \ ,\ i = 1,2,\dots,N \quad (26)$$
$$i = 1,2,\dots,N \text{ and } n = 1,2,\dots,N-1$$

To calculate higher-order derivatives, we will have:

$$[g^{(n)}] = [g^{(1)}][g^{(n-1)}] \quad (27)$$

The above relations are independent of the number and location of the sample points and on the other hand led to more accurate solutions due to the smaller error caused by rounding. In addition, the number of mathematical operations is also less and saves on calculation time. It is necessary to mention again that in this numerical method, unlike conventional numerical methods, adding the number of sample points does not necessarily lead to a better solution. This can be mentioned as one of the disadvantages of this method, but of course, considering the speed of convergence to the solution, this disadvantage can be ignored with a smaller number of sample points.

5. Calculation of mechanical properties of beam CNTRC

As you saw in Chapter 3, there are various methods for finding the mechanical properties of beams. There are CNTRC, among which we can mention the mixing law and the Eshelby-Mori-Tanaka method. It is worth noting that a number of articles have calculated mechanical properties using both methods, and in this Paper, the mixing law was used.

5.1. Method Eshel by-Mori-Tanaka

In this method, the stiffness matrix is calculated from the following equation:

$$C = C_m + V_{CNT}\left((C_{CNT} - C_m).A\right).[V_m I + V_{CNT}A]^{-1} \quad (28)$$
$$A = [I + S.C_m^{-1}.(C_{CNT} - C_m)]^{-1} \quad (29)$$

Which we have:

Stiffness matrix matrix C_m:

C_{CNT}: Hardness matrix of carbon nanotubes

I: Fourth-order unit tensor

S: Fourth-order Ashlabian tensor.

5.2. Mixing law

One of the most general and basic relationships used to determine the elastic modulus of composites is the mixing law. In this model, the filler is considered as long fibers and the Young's and shear moduli of the composite are obtained. In this model, the complete transfer of any stress applied to the system from the matrix material to the filler is assumed. For nanotube reinforced composites, the mixing law relationships are used with the difference that the efficiency parameters CNT, have been added to the equations. In Fig.6 the distribution of carbon nanotubes in the composite beam is shown. As is clearly seen, the first case is a uniform distribution and the other case is a non-uniform and functionally graded distribution.

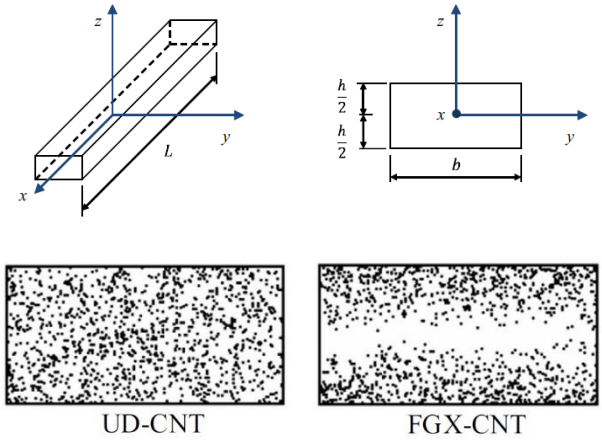

(a) (b)

Figure 6: Problem geometry and nanotube distribution in the beam CNTRC. (a) Uniform distribution. (b) Non-uniform and graded functional distribution

The relationships governing the shear and tensile moduli of a beam based on the mixing law are as follows:

$$E_{11} = \eta_1 V_{CNT}E_{11}^{CNT} + V_m E^m$$
$$\frac{\eta_2}{E_{22}} = \frac{V_{CNT}}{E_{22}^{CNT}} + \frac{V_m}{E^m} \quad (30)$$
$$\frac{\eta_3}{G_{12}} = \frac{V_{CNT}}{G_{12}^{CNT}} + \frac{V_m}{G^m}$$

Which:

$E_{11}{}^{CNT}, E_{22}{}^{CNT}, G_{12}{}^{CNT}$: Shear and tensile moduli of nanotubes

E^m, G^m: ModuleShear and tensile modulus of the matrix material

η_j $(j = 1,2,3)$: Nanotube efficiency coefficients

V_{CNT}, V_m: Volume fraction of matrix and nanotubes

It is worth noting that the effect of carbon nanotube size on the efficiency parameter definition CNT is considered, and this parameter is calculated by matching the results from molecular dynamics simulations and the mixing rule for the elastic modulus of CNTRCs.

As shown in Figure (1), each of the nanotube distribution states has its own volume fraction, which is obtained from the following relations:

$$V_{CNT} = V_{CNT}^{*} \qquad (UD\ CNTRC)$$
$$V_{CNT}(z) = \left(\frac{4|z|}{h}\right) V_{CNT}^{*} \qquad (FG - X\ \ CNTRC) \tag{31}$$

Which:

$$V_{CNT}^{*} = \frac{w_{CNT}}{w_{CNT} + (\rho^{CNT}/\rho^{m}) - (\rho^{CNT}/\rho^{m}) w_{CNT}} \tag{32}$$

Also, other properties of the beam CNTRC, including Poisson's ratio, density, coefficient of thermal expansion in the longitudinal direction, and coefficient of thermal expansion in the transverse direction, can be obtained similarly to other properties of the sheet as follows:

$$\begin{gathered} \nu_{12}\rho\alpha_{11}\alpha_{22} \\ \nu_{12} = V_{CNT}^{*}\,\nu_{12}^{CNT} + V_m \nu^m \\ \rho = V_{CNT}\rho^{CNT} + V_m\rho^m \\ \alpha_{11} = V_{CNT}\alpha_{11}^{CNT} + V_m\alpha^m \\ \alpha_{22} = (1+\nu_{12}^{CNT})V_{CNT}\alpha_{22}^{CNT} + (1+\nu^m)V_m\alpha^m \\ - \nu_{12}\alpha_{11} \end{gathered} \tag{33}$$

Which:

ν_{12}^{CNT} , ν^m: Poisson's ratio of matrix and nanotube

ρ^m , ρ^{CNT}: Nanotube density and matrix

α_{22}^{CNT} , α_{11}^{CNT}: Thermal expansion coefficient of the nanotube in the longitudinal and transverse directions, respectively

α^m: Matrix thermal expansion coefficient

The results of the mixing law are in very good agreement with the experimental results.

6. Extraction of state space equations

Without considering the volume forces, the equations of motion can be written as the following equation:

$$\begin{aligned} \sigma_{x,x} + \tau_{xz,z} &= \rho\frac{\partial^2 u}{\partial t^2} \\ \tau_{xz,x} + \sigma_{z,z} &= \rho\frac{\partial^2 w}{\partial t^2} \end{aligned} \tag{34}$$

in which σ_z and σ_x Axial stresses, τ_{xz} Shear stress, wandu Mechanical displacement in the transverse and axial directions, respectively, ρ Density of materials and t they are time. The relationship between strain and mechanical displacement for small deformations can be expressed as Equation 35.

$$\begin{aligned} \varepsilon_x &= \frac{\partial u}{\partial x} \\ \varepsilon_z &= \frac{\partial w}{\partial z} \\ \gamma_{xz} &= \frac{\partial u}{\partial z} + \frac{\partial w}{\partial x} \end{aligned} \tag{35}$$

That *u* and *w* Displacements and Normal strains in the direction of the coordinate axes, respectively *x* and *z* they are. Shear strain in the plane it is xz. Using Hooke's law and strain-displacement equations, the stress-displacement equations are obtained in the following form:

$$\begin{aligned} \sigma_x &= Q_{11}\frac{\partial u}{\partial x} + Q_{13}\frac{\partial w}{\partial z} \\ \sigma_z &= Q_{11}\frac{\partial u}{\partial x} + Q_{33}\frac{\partial w}{\partial z} \\ \tau_{xz} &= Q_{55}\left[\frac{\partial w}{\partial x} + \frac{\partial u}{\partial z}\right] \end{aligned} \tag{36}$$

That *Q11*, *Q33*, *Q13* and *Q55* they are calculated as follows:

$$\begin{gathered} Q_{11} = \frac{E_{11}}{\Delta}, \qquad Q_{33} = \frac{E_{33}}{\Delta}, \qquad Q_{13} = \nu_{31}\frac{E11}{\Delta}, \\ Q_{55} = G_{13} \\ \Delta = 1 - \nu_{31}\nu_{313} \end{gathered} \tag{37}$$

It should be noted that the degree of functional or homogeneity of a material is reflected in the stress-strain relationships. In a homogeneous material, the modulus of elasticity E is constant in all directions. Using equations (2) and (4), the state space equations are obtained in the following form:

$$\begin{aligned} \frac{\partial\sigma_z}{\partial z} &= -\frac{\partial\tau_{xz}}{\partial x} + \rho\frac{\partial^2 w}{\partial t^2} \\ \frac{\partial u}{\partial z} &= -\frac{\partial w}{\partial x} + \frac{1}{Q_{55}}\tau_{xz} \\ \frac{\partial w}{\partial z} &= \frac{1}{Q_{33}}\sigma_z - \frac{Q_{11}}{Q_{33}}\frac{\partial u}{\partial x} \\ \frac{\partial\tau_{xz}}{\partial z} &= -\frac{Q_{13}}{Q_{33}}\frac{\partial\sigma_z}{\partial x} - \left(Q_{11} - \frac{Q_{13}Q_{11}}{Q_{33}}\right)\frac{\partial^2 u}{\partial x^2} + \rho\frac{\partial^2 u}{\partial t^2} \end{aligned} \tag{38}$$

The boundary conditions for the various supports are as follows:

Simple support $\qquad \sigma_x = w = 0$ (39)

Free support $\sigma_x = \tau_{xz} = 0$

7. Analytical solution of a simply supported beam

First, the state space matrix is calculated for each layer, then the surface conditions between the layers and the continuity of stress and displacement are applied, and the overall state space matrix is obtained. Finally, by applying the surface conditions of the lower and upper surfaces (Equation 40), the equations are solved.

The surface conditions at the top and bottom surfaces of the beam are as follows:

$$\sigma_z = \tau_{xz} = 0, \qquad at\ z = -\frac{h}{2}, \frac{h}{2} \tag{40}$$

The boundary conditions at the simple support are as follows:

$$\sigma_x = w = 0, \qquad at\ x = 0, L \tag{41}$$

Considering the boundary conditions, the following Fourier expansions have been considered for stresses and displacements

$$\begin{aligned} u &= \sum_{m=1}^{\infty} \bar{U}(z)\cos(p_m x)e^{(i\omega t)} \\ w &= \sum_{m=1}^{\infty} \bar{W}(z)\sin(p_m x)e^{(i\omega t)} \\ \sigma_z &= \sum_{m=1}^{\infty} \bar{\sigma}_z(z)\sin(p_m x)e^{(i\omega t)} \\ \tau_{xz} &= \sum_{m=1}^{\infty} \bar{\tau}_{xz}(z)\cos(p_m x)e^{(i\omega t)} \\ \sigma_x &= \sum_{m=1}^{\infty} \bar{\sigma}_x(z)\sin(p_m x)e^{(i\omega t)} \end{aligned} \tag{42}$$

In the above relationship ωt the natural frequency of the beam and t is the time. By substituting the above equations into the state space equations (4-15), the following relations are obtained.

$$\begin{aligned} \frac{\partial \bar{\sigma}_z}{\partial z} &= p_m \bar{\tau}_{xz} - \rho\omega^2 \bar{W} \\ \frac{\partial \bar{U}}{\partial z} &= -p_m \bar{W} + \frac{1}{Q_{55}}\bar{\tau}_{xz} \\ \frac{\partial \bar{W}}{\partial z} &= \frac{1}{Q_{33}}\bar{\sigma}_z + \frac{Q_{11}}{Q_{33}} p_m \bar{U} \end{aligned} \tag{43}$$

Vector δ which includes state space variables is considered as follows.

$$\delta = \left\{ \bar{\sigma}_z \quad \bar{U} \quad \bar{W} \quad \bar{\tau}_{xz} \right\} \tag{44}$$

Using the defined vector, Equations (45) can be written in matrix form as follows.

$$\frac{d\delta}{dz} = G\delta \tag{45}$$

That G is defined as follows.

$$G = \begin{bmatrix} 0 & 0 & -\rho\omega^2 & p_m \\ 0 & 0 & -p_m & \frac{1}{Q_{55}} \\ \frac{1}{Q_{33}} & \frac{Q_{11}}{Q_{33}} p_m & 0 & 0 \\ -\frac{Q_{13}}{Q_{33}} p_m & (Q_{11} - \frac{Q_{13}Q_{11}}{Q_{33}}) p_m^2 - \rho\omega^2 & 0 & 0 \end{bmatrix} \tag{46}$$

The solution to the differential Equations (47) in matrix form is as follows.

$$\delta(z) = e^{\int_{z_0}^{z} G dz}\ \delta(z_0) \tag{47}$$

8. Semi-analytical solution of a beam with various supports using the differential square method

Initially, a semi-analytical solution is performed for the simple support and compared with the analytical solution presented in the previous section, which allows the best case for the number of sample points to be obtained.

To solve the semi-analytical state space equations, the beam is oriented in the direction *x* is discretized using the method of difference of squares with the help of *N* points:

$$x_i = \frac{L}{2}\left(1 - \cos\frac{(i-1)\pi}{N-1}\right) \tag{48}$$

in which xi is the length of the it *h* point and *L* is the total length of the beam. The derivatives with respect to x are discretized as follows:

$$\left(\frac{\partial^n f(x,z)}{\partial x^n}\right)_{x=x_i} = \sum_{j=1}^{N} A_{ij}^{(n)}\ f(x_j, z) \tag{49}$$

Values of the weight coefficients are calculated based on the Quan-Chang method according to the following formula:

$$\begin{aligned} A_{ij} &= \frac{1}{x_j - x_i} \prod_{j=1, r\neq i}^{N} \frac{x_i - x_r}{x_j - x_r}, \quad i \neq j \\ A_{ij} &= \sum_{r=1, r\neq i}^{N} \frac{1}{x_i - x_r}, \quad i = j \end{aligned} \tag{50}$$

In this case, the solution process is similar to the analytical case for a simple support, with the difference that

the dependence of the state space equations on the variables x and its derivatives are solved using the differential square method and the matrices that are calculated have much larger dimensions than the analytical solution. First, the state space matrix is calculated for each layer, then the boundary conditions between the layers and the continuity of stress and displacement are applied and the overall state space matrix is obtained. Finally, using the stress and displacement relationship of the upper and lower surfaces of the beam, the equations are solved.

Mode CS:

$$\begin{aligned} &u = w = 0, \quad \frac{\partial w}{\partial x} = 0, \qquad at\ x = 0 \\ &\sigma_x = w = 0, \qquad\qquad at\ x = L \end{aligned} \tag{51}$$

Mode CF:

$$\begin{aligned} &u = w = 0, \quad \frac{\partial w}{\partial x} = 0, \qquad at\ \ x = 0 \\ &\sigma_x = \tau_{xz} = 0, \qquad\qquad at\ x = L \end{aligned} \tag{52}$$

Mode CC:

$$\begin{aligned} &u = w = 0, \quad \frac{\partial w}{\partial x} = 0, \qquad at\ x = 0 \\ &u = w = 0, \quad \frac{\partial w}{\partial x} = 0, \qquad at\ x = L \end{aligned} \tag{53}$$

State space variables at a point(i)th are:

$$\delta_{(i)} = \left\{ \sigma_{z_{(i)}},\ \ u_{(i)},\ \ w_{(i)},\ \ \tau_{xz(i)} \right\}^{T} \tag{54}$$

According to Equation 54, the point state space equations are (i) will be as follows:

$$\frac{d\delta_{(i)}}{dz} = G_{(i)}\ \delta_{(i)} \tag{55}$$

By writing Equation 55 for different points in the solution domain, the system of total equations is obtained:

$$\frac{\partial \Delta}{\partial z} = M\Delta \tag{56}$$

In which, the matrix is called the general matrix and is defined as follows:

$$\Delta = \left\{ \sigma_z, u, w, \tau_{xz} \right\}^{T}_{1\times(6\times N)} \tag{57}$$

That:

$$\begin{aligned} \sigma_z &= \left\{ \sigma_{z_1}, \sigma_{z_2}, \ldots, \sigma_{z_{N_x\times N_y}} \right\}^{T}_{1\times N} \\ u &= \left\{ u_1, u_2, \ldots, u_{N_x\times N_y} \right\}^{T}_{1\times N} \\ w &= \left\{ w_1, w_2, \ldots, w_{N_x\times N_y} \right\}^{T}_{1\times N} \\ \tau_{xz} &= \left\{ \tau_{xz1}, \tau_{xz2}, \ldots, \tau_{xzN_x\times N_y} \right\}^{T}_{1\times N} \end{aligned} \tag{58}$$

Considering the removal of dependency M to x and its derivatives, the solution to Equation (57) can be easily obtained. But before that, boundary conditions in the x direction for the boundary points must be determined and applied. After applying the boundary conditions, the dimensions of the overall matrix are reduced and Equations (59) change to the following form.

$$\frac{\partial \Delta_b}{\partial z} = M\Delta_b \tag{59}$$

The analytical solution of Equations 59 is as follows:

$$\Delta_b = e^{\int_{z_0}^{z} M_b z} \left\{ c \right\} \tag{60}$$

that the column matrix constants *C* column vector value It is at the bottom of the layer.

9. Applying surface conditions to the upper and lower surfaces

According to Equation 60, it can be written:

$$\begin{bmatrix} \bar{\sigma}_z(h/2) \\ \bar{U}(h/2) \\ \bar{W}(h/2) \\ \bar{\tau}_{xz}(h/2) \end{bmatrix} = \begin{bmatrix} s_{11} & s_{12} & s_{13} & s_{14} \\ s_{21} & s_{22} & s_{23} & s_{24} \\ s_{31} & s_{32} & s_{33} & s_{34} \\ s_{41} & s_{42} & s_{43} & s_{44} \end{bmatrix} \begin{bmatrix} \bar{\sigma}_z(-h/2) \\ \bar{U}(-h/2) \\ \bar{W}-(h/2) \\ \bar{\tau}_{xz}(-h/2) \end{bmatrix} \tag{61}$$

Which we will have by applying boundary conditions.

$$\begin{bmatrix} 0 \\ \bar{U}(h/2) \\ \bar{W}(h/2) \\ 0 \end{bmatrix} = \begin{bmatrix} s_{11} & s_{12} & s_{13} & s_{14} \\ s_{21} & s_{22} & s_{23} & s_{24} \\ s_{31} & s_{32} & s_{33} & s_{34} \\ s_{41} & s_{42} & s_{43} & s_{44} \end{bmatrix} \begin{bmatrix} 0 \\ \bar{U}(-h/2) \\ \bar{W}-(h/2) \\ 0 \end{bmatrix} \tag{62}$$

The previous equations are solved by removing unnecessary rows and columns.

$$\begin{bmatrix} 0 \\ 0 \end{bmatrix} = \begin{bmatrix} s_{12} & s_{13} \\ s_{42} & s_{43} \end{bmatrix} \begin{bmatrix} \bar{U}(-h/2) \\ \bar{W}(-h/2) \end{bmatrix} \tag{63}$$

To analyze the free vibrations of the beam, considering that the left side of Equations 63 becomes zero, the natural frequencies of the beam have been calculated by setting the determinants of the coefficients equal.

The natural frequencies in the analytical solution are calculated using the following equation.

$$\left| S_A \right| = 0 \tag{64}$$

The natural frequencies in the semi-analytical solution are calculated using the following equation.

$$\left| S_D \right| = 0 \tag{65}$$

To demonstrate the accuracy and precision of the calculations in the previous chapter, numerical results are presented in the form of graphs and tables for various

problems and materials in this chapter. The results include the calculation of the natural frequency of the nanocomposite beam FG, which has been validated according to the results in authoritative papers. First, the convergence of the numerical solution (DQ) for a simple support is shown and compared with the analytical solution. Then, to ensure the accuracy and precision of the method used, the results for different boundary conditions are compared and validated with authoritative papers. Next, the effect of the dimensions and percentage of nanotube presence (V*CNT) on the natural frequencies is investigated and their results are presented for comparison. In Table 1, the values of nanotube efficiency (iη) are shown for the studied nanocomposite beams.

Table 1
Nanotube efficiency values ($I\eta$)

CNT efficiency parameters	VCNT		
	0.12	0.17	0.28
1η	1.2833	1.3414	1.3238
2η	1.0556	1.7101	1.7380
3η	1.0556	1.7101	1.7380

10. Solution convergence DQ and comparison with analytical solution

In this section, the convergence of the differential square solution with increasing number of sample points is investigated and compared with the analytical solution. In Table 2, the first three modes of natural frequencies for a uniform distribution of nanotubes (UD) and functional graded distribution (FG-X) are presented. The frequencies presented in the table are for a nanocomposite beam with simply supported SS boundary conditions. According to the table, at the number of sample points of 9 and 10, the results of the semi-analytical solution have good convergence, and it is also seen that with increasing the vibration mode, the number of sample points of convergence increases. It is observed that the numerical solution provides very fast and good convergence, and its results are very close to the results of the analytical solution.

Table 2
Convergence of the results of the first three modes of natural frequencies in the numerical solution and comparison with the analytical solution

Mode	Method	UD	FG-X
1	DQM (N=5)	1.2243	1.3575
	(N=6)	1.2284	1.3619
	(N=7)	1.2287	1.3621
	(N=8)	1.2287	1.3621
	(N=9)	1.2287	1.3621
	Exact	1.2290	1.3624
2	DQM (N=5)	3.656	3.8071
	(N=6)	3.1823	3.3353
	(N=7)	3.2402	3.3929
	(N=8)	3.2383	3.3910
	(N=9)	3.2384	3.3912
	Exact	3.2384	3.3914
3	DQM (N=5)	4.8918	5.0376
	(N=6)	4.9453	5.1269
	(N=7)	5.0769	5.2219
	(N=8)	5.2929	5.4372
	(N=9)	5.2646	5.4089
	(N=10)	5.2700	5.4130
	Exact	5.2675	5.4121

11. Validation of the problem-solving method

In this section, the accuracy of the presented solution is examined and validation is performed. For this purpose, the problem conditions that are described in the articles [31] and [32] have been considered and the numerical results of the present study have been compared with the results of the aforementioned articles. Table 3 shows the changes of the first mode of the dimensionless natural frequency for simple-simple (SS), simple-clamped (CS) and clamped-clamped (CC) supports. The results in this table have been considered in two completely analytical and numerical (DQ) methods for the simple support and in the numerical (DQ) method for the other supports. A comparison can be made between the results obtained from the analytical solution, the numerical solution and the results of the aforementioned articles. The results presented; compliance it shows a very good agreement between the two methods used.

12. Effect of various boundary conditions on natural frequency

To better compare the effect of boundary conditions on beam behavior, the first four dimensionless natural frequency modes for different boundary conditions are shown together in Table 4.

Table 3
First mode dimensionless natural frequency for simple-simple (SS), simple-clamped (CS) and clamped-clamped (CC) supports and comparison with the results of papers [31] and [32]

CNT distribution	Boundary conditions	Present Perfect	Present DQM	Reference [1]	Reference [2]
UD-CNT	CC	-	1.6817	1.6691	1.6678
	CS	-	1.4495	1.4565	1.4556
	SS	1.229	1.2287	1.2581	1.2576
FGX-CNT	CC	-	1.7477	1.7242	1.7230
	CS	-	1.5414	1.5394	1.5385
	SS	1.3624	1.3621	1.3859	1.3852

Table 4
The first four dimensionless natural frequency modes for different boundary conditions

BC	Mode			
	1	2	3	4
CF	0.5727	2.1128	4.2359	6.3008
SS	1.3624	3.3914	5.4121	7.4261
CS	1.5414	3.4651	5.4543	7.5711
CC	1.7477	3.5353	5.5040	7.6071

According to Table 4, the stiffer or more restricted the plate is in the support, the higher the natural frequency it will have. In the case CC has the highest natural frequency and CF has the lowest natural frequency.

13. The effect of length to thickness ratio (L/h) at natural frequencies

At this stage, the aim is to investigate the effect of the length to thickness ratio (L/h) in the dimensionless natural frequency of a nanocomposite beam with nanotube distribution FG-X. In Figure 7, the changes in the dimensionless natural frequency as a function of the ratio (L/h) for the FG-X nanocomposite beam can be seen. With increasing L/h, the natural frequency increases, and at low values, the changes in the natural frequency are very severe.

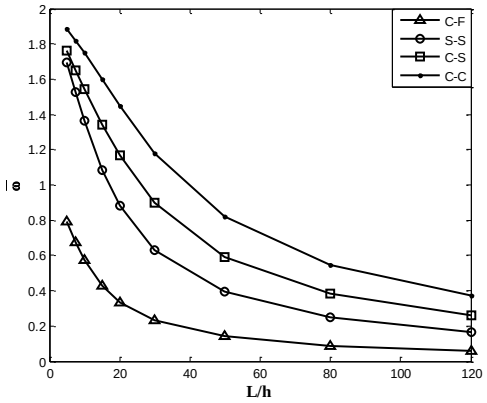

Figure 7: Variations of dimensionless natural frequency in terms of ratio (L/h) for FG-X nanocomposite beam

14. The effect of the volume fraction of the presence of nanotubes (V*CNT) in nanocomposite beam

At this stage, the aim is to investigate the effect of the volume fraction of the presence of nanotubes (V*CNT) in the natural frequency of the FG-X and UD nanocomposite beam. With increasing V*CNT, the percentage of mixing method and, in the direction of thickness, the numerical method of differential quadrature DQ and the nanotubes increases. Tables 5, 6, 7 and 8 show the changes in the first three modes of the dimensionless natural frequency of the beam with CC, CS, SS and CF supports in terms of V*CNT, respectively. It is observed that with increasing the V*CNT parameter, the dimensionless natural frequency increases.

Table 5
Variations of the first three modes of the dimensionless natural frequency of the beam with CC supports in terms of V*CNT(L/h=20)

V*CNT		Mode		
		1	2	3
0.12	UD	1.6817	3.4196	5.3825
	FG-X	1.7477	3.5353	5.5040
0.17	UD	2.1524	4.3955	6.9415
	FG-X	2.2368	4.5264	7.0914
0.28	UD	2.3796	4.8195	7.5578
	FG-X	2.4299	4.9131	7.6625

Table 6
Variations of the first three modes of the dimensionless natural frequency of the beam with CS supports in terms of V*CNT(L/h=20)

V*CNT		Mode		
		1	2	3
0.12	UD	1.0351	2.6928	4.6294
	FG-X	1.1674	2.9170	4.8939
0.17	UD	1.2817	3.3878	5.8838
	FG-X	1.4518	3.6784	6.2224
0.28	UD	1.6807	4.1134	6.8294
	FG-X	2.1597	4.8186	7.6215

Table 7
Variations of the first three modes of the dimensionless natural frequency of the beam with SS supports in terms of V*CNT(L/h=20)

V*CNT		Mode		
		1	2	3
0.12	UD	0.7536	2.4580	4.4434
	FG-X	0.8842	2.7247	4.7494
0.17	UD	0.9203	3.0632	5.6188
	FG-X	1.0839	3.4085	6.0155
0.28	UD	1.1262	3.5825	6.3696
	FG-X	1.3053	3.8759	6.6379

Table 8
Variations of the first three modes of the dimensionless natural frequency of the beam with CF supports in terms of V*CNT(L/h=20)

V*CNT		Mode		
		1	2	3
0.12	UD	0.3361	1.6040	3.5326
	FG-X	0.2814	1.4311	3.2575
0.17	UD	0.3416	1.7765	4.0979
	FG-X	0.4092	1.9990	4.4523
0.28	UD	0.4237	2.0963	4.6998
	FG-X	0.5033	2.3040	4.9895

15. Conclusion

In this research to the vibration analysis of a Nano-beam unidirectional FGM (functional properties along the beam thickness) with carbon nanotubes and a Layer-Metal and ceramic braces on various supports w whether simple, complex, etc. became. The solution method used is the assumptions in this research in this way it is that the material properties change along the thickness as an

exponential function slow, the beam is under plane tension, no there is no thickness variation or discontinuity in the longitudinal direction of the beam, Poisson's ratio in the layer FGM is constant along its thickness. Accordingly, the following results have been obtained:

1. The stiffer, or more constrained, the sheet in the support will have a higher natural frequency.
2. In the state CC has the highest natural frequency and CF has the lowest natural frequency.
3. By increasing the length to thickness ratio L/h the natural frequency increases.
4. When the length to thickness ratio is low, the natural frequency changes are very severe.
5. By increasing the volume fraction parameter of the presence of nanotubes V*CNT increases the dimensionless natural frequency.
6. In the case where the volume fraction of nanotubes in the beam FGM is fixed, relying sometimes YRadar-GYRadar has the highest natural frequency in all modes.
7. In the case where the volume fraction of nanotubes in the beam FGM is fixed, relying sometimes YRadar-free has the lowest natural frequency of all modes.
8. In any case of the volume fraction of nanotubes in the beam FGM the first mode has the lowest frequency and subsequent modes have a higher frequency than the previous mode.

References

[1] Ichikawa, Kiyoshi, ed. Functionally graded materials in the 21st century: a workshop on trends and forecasts. Springer Science & Business Media, 2001.26-28. DOI: 10.1007/978-1-4615-4373-2

[2] Suresh, Subra, and Andreas Mortensen. “Fundamentals of Functionally Graded Materials.” London: IOM Communications Ltd., 1998.

[3] Sankar, B.V. “An elasticity solution for functionally graded beams.” Composites Science and Technology 61.5 (2001): 689–696. DOI: https://doi.org/10.1016/S0266-3538(01)00007-0.

[4] Chakraborty, A., and S. Gopalakrishnan. “A spectrally formulated finite element for wave propagation analysis in functionally graded beams.” International Journal of Solids and Structures 40.10 (2003): 2421–2448. DOI: https://doi.org/10.1016/S0020-7683(03)00029-5.

[5] Chakraborty, A., S. Gopalakrishnan, and J.N. Reddy. “A new beam finite element for the analysis of functionally graded materials.” International Journal of Mechanical Sciences 45.3 (2003): 519–539. DOI: https://doi.org/10.1016/S0020-7403(03)00058-4.

[6] Shi, Z.F., and Y. Chen. “Functionally graded piezoelectric cantilever beam under load.” Archive of Applied Mechanics 74.3–4 (2004): 237–247. DOI: https://doi.org/10.1007/BF02637199.

[7] Ding, H. J., D. J. Huang, and WQ2304402 Chen. "Elasticity solutions for plane anisotropic functionally graded beams." International Journal of Solids and Structures 44.1 (2007): 176-196. https://doi.org/10.1016/j.ijsolstr.2006.04.026

[8] Kapuria, S., M. Bhattacharyya, and A.N. Kumar. “Bending and free vibration response of layered functionally graded beams: A theoretical model and experimental validation.” Composite Structures 82.3 (2008): 390–402. DOI: https://doi.org/10.1016/j.compstruct.2007.01.019 .

[9] Kadoli, Ravikiran, Kashif Akhtar, and N. Ganesan. “Static analysis of functionally graded beams using higher order shear deformation theory.” Applied Mathematical Modelling 32.12 (2008): 2509–2525. DOI: https://doi.org/10.1016/j.apm.2007.09.015 .

[10] Li, X.F. “A unified approach for analyzing static and dynamic behaviors of functionally graded Timoshenko and Euler–Bernoulli beams.” Journal of Sound and Vibration 318.4–5 (2008): 1210–1229. DOI: https://doi.org/10.1016/j.jsv.2008.04.017 .

[11] Tao, Yu, and Zhong Zheng. “Bending analysis of a functionally graded piezoelectric cantilever beam.” Science in China Series G: Physics, Mechanics & Astronomy 50.1 (2007): 97–108. DOI: https://doi.org/10.1007/s11433-007-2006-6 .

[12] Huang, De-jin, Hao-jiang Ding, and Wei-qiu Chen. “Analytical solution for functionally graded anisotropic cantilever beam subjected to linearly distributed load.” Applied Mathematics and Mechanics 28.7 (2007): 855–860. DOI: https://doi.org/10.1007/s10483-007-0702-1.

[13] Huang, De-jin, Hao-jiang Ding, and Wei-qiu Chen. “Analytical solution for functionally graded anisotropic cantilever beam under thermal and uniformly distributed load.” Journal of Zhejiang University-SCIENCE A 8.9 (2007): 1351–1355. DOI: https://doi.org/10.1631/jzus.2007.A1351.

[14] Ying, Ji, Chuan-Fu Lu, and Wei-Qiu Chen. “Two-dimensional elasticity solutions for functionally graded beams resting on elastic foundations.” Composite Structures 84.3 (2008): 209–219. DOI: https://doi.org/10.1016/j.compstruct.2006.12.004.

[15] Zhong, Zhihong, and Tianyu Yu. “Analytical solution of a cantilever functionally graded beam.” Composites Science and Technology 67.3–4 (2007): 481–488. DOI: https://doi.org/10.1016/j.compscitech.2006.08.023.

[16] Ding, Hao-jiang, De-jin Huang, and Wei-qiu Chen. “Elasticity solutions for plane anisotropic functionally graded beams.” International Journal of Solids and Structures 44.1 (2007): 176–196. DOI: https://doi.org/10.1016/j.ijsolstr.2006.04.036.

[17] Farhatnia, Farhad, Ghasem Sharifi, and Sadegh Rasouli. “Numerical and analytical approach of thermo-mechanical stresses in FGM beams.” Proceedings of the World Congress on Engineering 2 (2009): [No page range]. DOI: Not available.

[18] Alibeigloo, Akbar. “Thermoelasticity analysis of functionally graded beam with integrated surface piezoelectric layers.” Composite Structures 92.7 (2010): 1535–1543. DOI: https://doi.org/10.1016/j.compstruct.2009.10.015.

[19] Simsek, Mehmet. “Fundamental frequency analysis of functionally graded beams by using different higher-order beam theories.” Nuclear Engineering and Design 240.4 (2010): 697–705. DOI: https://doi.org/10.1016/j.nucengdes.2009.12.013.

[20] Thai, Hoc, and Tuan Vo. “Bending and free vibration of functionally graded beams using various higher-order shear deformation beam theories.” Nuclear Engineering and Design 262 (2012): 57–66. DOI: https://doi.org/10.1016/j.nucengdes.2013.03.001.

[21] Pradhan, Krishna, and Snehashish Chakraverty. “Free vibration of Euler and Timoshenko functionally graded beams by Rayleigh-Ritz method.” Composites Part B: Engineering 51 (2013): 175–184. DOI: https://doi.org/10.1016/j.compositesb.2013.02.030.

[22] Thomas, Biju, Pravin Inamdar, Tapas Roy, and B. K. Nada. “Finite element modeling and free vibration analysis of functionally graded nanocomposite beam reinforced by randomly oriented carbon nanotubes.” International Journal of Theoretical and Applied

Research in Mechanical Engineering 2 (2013): 2319–3182. DOI: Not available.

[23] Mohammadimehr, Mohammad, and Mahdi Mahmudian. “Bending and free vibration analysis of nonlocal functionally graded nanocomposite Timoshenko beam model reinforced by SWBNNT based on modified coupled stress theory.” Journal of Nanostructures 3.4 (2013): 483–492. DOI: Not available.

[24] Heshmati, Mohammad, and Mohammad Yas. “Free vibration analysis of functionally graded CNT-reinforced nanocomposite beam using Eshelby-Mori-Tanaka approach.” Journal of Mechanical Science and Technology 27.11 (2013): 3403–3408. DOI: https://doi.org/10.1007/s12206-013-0857-4.

[25] Moradi-dastjerdi, Reza, Gholamreza Payganeh, and Hamed Malek-mohammadi. “Free vibration analysis of functionally graded CNT-reinforced nanocomposite sandwich plates resting on elastic foundation.” Journal of Solid Mechanics 7.2 (2015): 158–172. DOI: Not available.

[26] Bellman, Richard, and John Casti. “Differential quadrature and long-time integration.” Journal of Mathematical Analysis and Applications 235.2 (1997): 235–238. DOI: https://doi.org/10.1006/jmaa.1997.5717.

[27] Bellman, Richard, B. G. Kashef, and John Casti. “Differential quadrature: A technique for the rapid solution of nonlinear partial differential equations.” Journal of Computational Physics 10.1 (1972): 40–52. DOI: https://doi.org/10.1016/0021-9991(72)90045-9.

[28] Hu, Li-Chung, and Chin-Rong Hu. “Identification of rate constants by differential quadrature in partially measurable compartmental models.” Mathematical Biosciences 21.1 (1974): 71–78. DOI: https://doi.org/10.1016/0025-5564(74)90054-5.

[29] Civan, Faruk, and Charles M. Sliepcevich. “Application of differential quadrature to transport processes.” Journal of Mathematical Analysis and Applications 93.1 (1983): 206–221. DOI: https://doi.org/10.1016/0022-247X(83)90116-0.

[30] Naadimuthu, G., Richard Bellman, and K. M. Wang. “Differential quadrature and partial differential equation: Some numerical results.” Acta Mechanica 24.1 (1995): 85–94. DOI: https://doi.org/10.1007/BF01176994.

[31] Yas, Mohammad Hossein, and Nima Samadi. “Free vibration and buckling analysis of carbon nanotube-reinforced composite Timoshenko beam on elastic foundation.” International Journal of Pressure Vessels and Piping 98 (2012): 119–128. DOI: https://doi.org/10.1016/j.ijpvp.2012.07.003.

[32] Yang, Liao-Liang, and Supachai Kitipornchai. “Nonlinear free vibration of functionally graded carbon nanotube-reinforced composite beams.” Composite Structures 92.3 (2010): 676–683. DOI: https://doi.org/10.1016/j.compstruct.2009.09.004.

[33] Zarehparvar-Shoja, Mohammad, Reza Shadnia, and Amin Kazemi Beydokhti. “Physical and chemical surface modifiers of carbon nanotubes on the mechanical and physical properties of concrete.” Journal of Civil Engineering Researchers 7.1 (2025): 34–47. DOI: https://doi.org/10.61186/JCER.7.1.34.